

Iron oxide nanozyme catalyzed synthesis of fluorescent polydopamine for light-up Zn²⁺ detection

Biwu Liu, Xiao Han, and Juewen Liu*

Department of Chemistry, Waterloo Institute for Nanotechnology,
University of Waterloo, Waterloo, Ontario, Canada, N2L 3G1.

Email: liujw@uwaterloo.ca

Abstract

Fluorescent polydopamine (FPD) is an interesting material with excellent biocompatibility. However, its preparation is currently a lengthy and potentially dangerous process. We herein employ magnetic iron oxide (Fe_3O_4) nanoparticles as a peroxidase-mimicking nanozyme to produce FPD under mild conditions. Different from previous protocols using multiple steps with up to 6% (~ 2 M) H_2O_2 , this preparation takes place in a single step with just 5 mM H_2O_2 at room temperature. The oxidized product shows excitation-wavelength-dependent emission peaks, similar to previous reports. The reaction kinetics, pH, temperature, and ionic strength are individually optimized. Among a diverse range of other nanomaterials tested, including Fe_2O_3 , CeO_2 , CoO , Co_3O_4 , NiO , TiO_2 , gold nanoparticles, and graphene oxide, Fe_2O_3 and graphene oxide also yielded relatively weak emission, while the rest of the materials failed to produce FPD. The Fe_3O_4 nanoparticles retained $\sim 90\%$ catalytic activity even after ten cycles of synthesis. Finally, Zn^{2+} can enhance the fluorescence of FPD under 360 nm excitation but not under 480 nm excitation, leading to a sensitive light-up sensor with a detection limit of 60 nM Zn^{2+} . Therefore, this work has demonstrated not only a novel use of nanozyme, but also an interesting application for FPD.

Introduction

Dopamine is a well-known neurotransmitter. Aside from its biological importance, it is also an intriguing molecule far from being fully understood. Dopamine can be oxidized and polymerized in alkaline conditions to form polydopamine.^{1,2} Due to its excellent biocompatibility, polydopamine has been extensively investigated for surface coating,² molecular imprinting,³ and biosensing.⁴ Recently, polydopamine was found to be fluorescent under certain conditions. For example, Zhang and co-workers obtained fluorescent polydopamine (FPD) nanoparticles (NPs) by treating polydopamine with concentrated H_2O_2 .⁵ The resulting FPD exhibited excitation-wavelength-dependent emission, and it was used for cell imaging. Using a similar method, FPD capsules were formed on SiO_2 and CaCO_3 templates.⁶ Yildirim et al. determined that FPD is an intermediate during the dopamine auto-oxidation process in alkaline conditions.⁷ Hydroxyl radicals generated by the Fenton agent (Fe^{2+} - H_2O_2) was also effective in degrading polydopamine.⁸ However, all these methods require concentrated H_2O_2 (e.g. up to 6%). The resulting harmful free radicals may limit the application of FPD, and concentrated H_2O_2 also poses a safety hazard.

The involvement of H_2O_2 for producing fluorescent materials suggests a possibility of accelerating the reaction by using a peroxidase. Nanozymes are nanomaterials with enzyme-like activities.⁹⁻¹² Noble metals,¹³⁻¹⁵ carbons,¹⁶⁻¹⁸ and metal oxides¹⁹⁻²⁴ have been demonstrated to mimic oxidase, peroxidase, catalase, and/or superoxide dismutase enzymes. Among these nanozymes, iron oxide is particularly interesting due to its unique magnetic property.^{20,25-27} Since the first report by Yan and co-workers,²⁰ iron oxide peroxidase nanozymes have been extensively studied. Some applications include the

detection of H₂O₂ and glucose,²⁷ nerve agents,²⁵ and Ebola virus.²⁸ To assay the peroxidase-like activity of iron oxide NPs, chromogenic substrates were commonly used. Dopamine was also used as such a substrate.^{29,30} Typically, the reaction is carried out at low pH, and oxidized dopamine appears yellow. However, no fluorescence was reported for such products. Therefore, we are interested in testing a new application of iron oxide nanozymes in this work: preparing FPD under milder conditions. We also report that FPD can be used for highly sensitive Zn²⁺ detection.

Materials and Methods

Chemicals. Dopamine hydrochloride, hydrogen peroxide (30 wt%), 3,3',5,5'-tetramethylbenzidine (TMB), iron(III) chloride, iron(II) chloride, cobalt(II) chloride, nickel chloride, copper sulfate, zinc chloride, manganese(II) chloride, lead acetate, and mercury chloride were acquired from Sigma-Aldrich (St. Louis, MO, USA). Sodium acetate, 4-(2-hydroxyethyl) piperazine-1-ethanesulfonic acid (HEPES), sodium acetate, 4-(2-hydroxyethyl) piperazine-1-ethanesulfonic acid (HEPES), 2-(N-morpholino) ethanesulfonic acid (MES) were from Mandel Scientific (Guelph, ON, Canada).were from Mandel Scientific (Guelph, ON, Canada). Nanoceria dispersion (catalog number 289744, 20 wt % dispersed in 2.5% acetic acid), Fe₃O₄ NPs (< 50 nm, catalog number 637106), and TiO₂ NPs (25 nm, catalog number 637254) were purchased from Sigma. CoO (50 nm, US3051), Co₃O₄ (10-30 nm, US3056), NiO (10-20 nm, US3356) were from US Nano Research. Citrate-capped AuNPs (~13 nm) were prepared based on literature.³¹ Graphene oxide (GO) was purchased from ACS Material, LLC (Medford, MA, USA). Milli-Q water was used for all of the experiments.

Instrumentation. The UV-vis absorption spectra were recorded on an UV-vis spectrometer (Agilent 8453A). The transmission electronic microscopy was performed using a Philips CM10 microscope. The fluorescence measurements were carried out using a Varian Eclipse fluorescence spectrometer (Agilent Technologies, Santa Clara, CA).

Preparation of FPD. In a typical synthesis, freshly prepared dopamine (0.5 mM) was incubated with H₂O₂ (5 mM) in the presence of Fe₃O₄ NPs (0.5 mg/mL) in the acetate buffer (pH 4, 50 mM) for 2 h. Occasional vortex was performed to avoid the precipitation of Fe₃O₄ NPs. After separating Fe₃O₄ NPs by a magnet, the supernatant containing FPD was collected for further measurement. The kinetics of fluorescence generation was recorded by measuring the fluorescent spectra of the supernatant at designated time points.

Effect of nanomaterials. The dopamine oxidation in the presence of different nanomaterials was carried out in a similar way. The concentration of metal oxide NPs was 0.5 mg/mL, AuNPs 5 nM, and GO 0.1 mg/mL. After 2 h reaction, the nanomaterials were separated by centrifugation (15 000 rpm, 15 min) and the supernatant was collected for further measurement.

Optimization of synthesis. The pH effect was investigated by incubating dopamine, Fe₃O₄ NPs, and H₂O₂ at pH 4 (acetate buffer), pH 5 (acetate buffer), pH 6 (MES buffer), pH 7 (HEPES buffer), pH 8 (HEPES buffer), and pH 8.5 (Tris buffer) for 2 h. The buffer concentration was 50 mM. The effect of ionic strength was examined by adding NaCl to the buffer solution (pH 4 acetate buffer, 50 mM). The fluorescence spectra after 2 h reaction were recorded. To test the temperature effect, the reaction mixture was incubated at different temperatures (4 °C in a fridge, 15 -65 °C in a water bath). After 1 h reaction, the fluorescence spectra were recorded.

Stability of FPD. The stability was examined by respectively incubating the prepared FPD at different pH (4, 5, 6, 7, 7.6, and 8.5), NaCl concentration (0, 50, 100, 250, and 500 mM), and divalent metal ions (Mg^{2+} , Ca^{2+} , Sr^{2+} , Ba^{2+} , 1 mM each) overnight. Typically, 50 μL of the prepared FPD in acetate buffer (10 mM, pH 4) was added into 50 μL of buffer solutions (100 mM) with designed pH or salt. The fluorescence spectra were then recorded.

Zn^{2+} detection. To test metal selectivity, 50 μL of the prepared FPD was respectively incubated with various metal ions (10 μM each), including Fe^{3+} , Fe^{2+} , Co^{2+} , Ni^{2+} , Cu^{2+} , Zn^{2+} , Mn^{2+} , Pb^{2+} , and Hg^{2+} in HEPES buffer (pH 7.6, 50 mM). The fluorescence emission spectra were recorded under two excitation wavelengths (360 nm and 480 nm). To test the sensitivity for Zn^{2+} detection, 20 μL of FPD was mixed with different concentrations of Zn^{2+} in HEPES buffer (pH 7.6, 50 mM). After 3 min, the fluorescence intensity at 500 nm (excitation at 360 nm) was recorded.

Results and Discussion

Synthesis of FPD with Fe_3O_4 nanozyme.

So far, only a few papers reported the synthesis of fluorescent polydopamine (FPD). While these protocols vary quite a bit, they generally involve two steps. 1) Polymerizing dopamine into polydopamine under basic conditions. In this process, dopamine is oxidized by oxygen. 2) H_2O_2 is then added to further oxidize or break polydopamine to FPD. This step often employs a high concentration (e.g. 6% or $\sim 2\text{ M}$) of H_2O_2 .⁵ Therefore, it is desirable to reduce the H_2O_2 concentration during the synthesis. In the past decade, it has become clear that iron oxide NPs are efficient peroxidase mimicking nanozymes. We

hypothesize that by providing a nanozyme surface for localized oxidation, one-step synthesis of FPD might be achieved as depicted in Figure 1A.

To test this idea, dopamine was incubated with H_2O_2 in the presence of Fe_3O_4 NPs. Our Fe_3O_4 NPs have an average size of 25 nm as indicated by TEM (Figure S1). After overnight incubation at room temperature, a yellow color was developed (inset of Figure 1B), suggesting oxidation of dopamine.^{1,29} The sample was characterized by UV-vis absorption spectroscopy, and a peak centered at 450 nm was obtained (Figure 1B, blue curve). Control samples of free dopamine, dopamine with H_2O_2 alone, and dopamine mixed with Fe_3O_4 NPs alone were also prepared. No color change or absorption peaks in the visible region were found for these control samples. It needs to be pointed out that we used only 5 mM H_2O_2 here, which is ~400-fold lower compared to the previous reported methods (6% $\text{H}_2\text{O}_2 = 1.96 \text{ M}$).⁵

The oxidation of dopamine by H_2O_2 using natural protein enzymes or nanozymes was observed by several groups.^{29,32} However, none of these papers mentioned the fluorescence property of the oxidation products. For the four samples we prepared above, a green/yellow fluorescence was observed for the one with both H_2O_2 and Fe_3O_4 NPs when excited at 470 nm (inset of Figure 1C). We also recorded the fluorescence spectra, and this sample showed an emission peak at 530 nm (Figure 1C, excitation 480 nm). When excited at different wavelengths, the emission peaks were also shifted accordingly (Figure 1D). This result is similar to the FPD reported by other groups.^{5,7,8} Such a property suggests the complexity of dopamine oxidation by H_2O_2 , yielding a mixture. Each type of molecule in this mixture has its own optimal excitation and emission wavelength, which is likely due to the different degree of polymerization. The strongest emission was obtained when

exciting the sample at 480 nm (Figure S2). All the control samples failed to show any fluorescence. Therefore, the Fe_3O_4 nanozyme can indeed achieve one-pot production of FPD under mild conditions. We characterized our FPD using TEM (Figure S3). Particles from a few to 15 nm were observed, consistent with a broad size distribution from the above fluorescence characterization. The quantum yield of our FPD is 1.0% (Figure S4), which is similar to the value (1.2%) reported by Lin et al.⁸

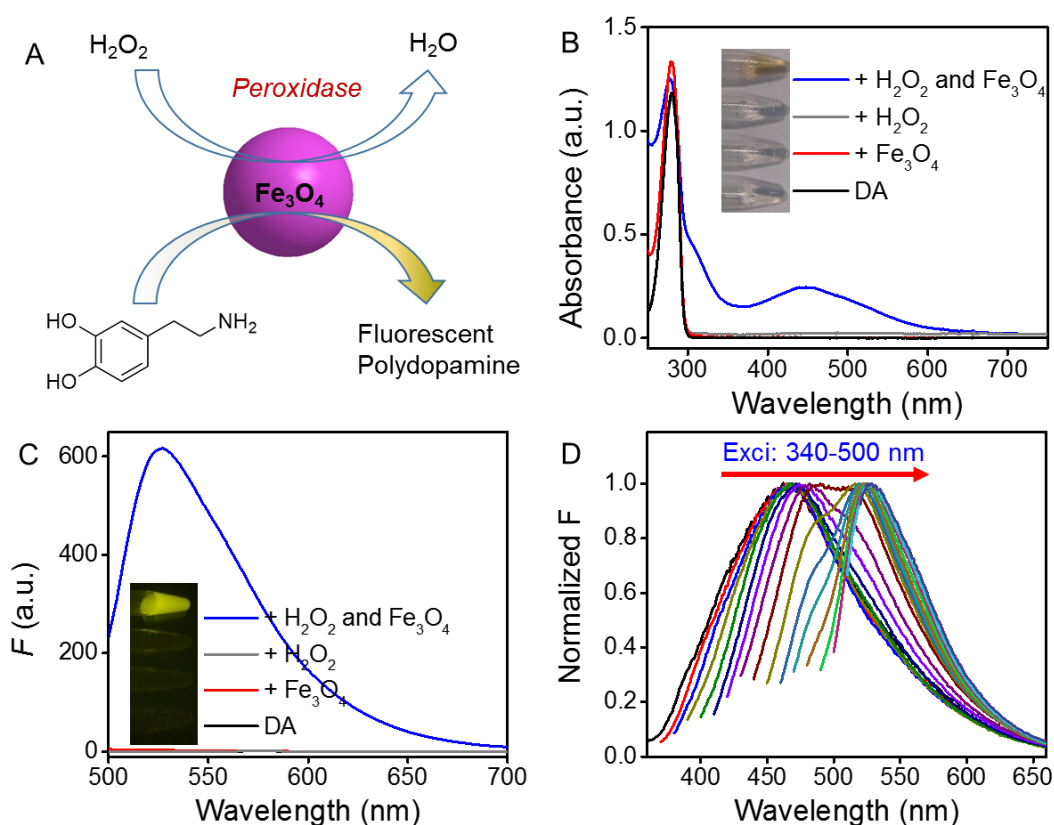


Figure 1. (A) Schematic representation of preparation of FPD using Fe_3O_4 NPs as a peroxidase mimicking nanozyme. (B) UV-vis absorption and (C) fluorescence emission spectra (excitation at 480 nm) of our prepared FPD and the control samples omitting H_2O_2 or Fe_3O_4 or both. DA = dopamine. The inset photographs are the dopamine samples (B)

under ambient light, and (C) under 470 nm LED excitation in a dark room. (D) Normalized FPD emission spectra at various excitation wavelengths.

Effect of other nanozymes

Many inorganic NPs have been reported to possess peroxidase-like activity.¹⁰ We chose Fe₃O₄ since it is a well-known peroxidase mimic with magnetic property. Similar to Fe₃O₄, Fe₂O₃ can also catalyze dopamine peroxidation and the product is fluorescent (Figure S5). To test if other NPs can also be used, we next carried the reaction in the presence of a few common nanomaterials, including CeO₂, CoO, Co₃O₄, NiO, TiO₂, gold nanoparticles (AuNPs), and graphene oxide (GO). Two nanozyme activities were respectively assayed: oxidase and peroxidase. Both assays used the same chromogenic substrate, 3,3',5,5'-tetramethylbenzidine (TMB). CeO₂, CoO, and NiO induced TMB oxidation in the absence of H₂O₂ and thus they are oxidase mimics (Figure 2A). Similarly, these three metal oxides also oxidized dopamine in the absence of H₂O₂, as indicated by the yellow color (Figure 2B, Figure S6A). However, such oxidized products are non-fluorescent (Figure 2C,D).

All these materials (except for TiO₂) catalyzed TMB oxidation in the presence of H₂O₂ (Figure 2E), suggesting that they are peroxidase mimics. Indeed, these peroxidase mimics also catalyzed the peroxidation of dopamine (Figure 2F, Figure S6B). Fluorescence measurement, however, showed that only GO and Fe₃O₄ NPs yielded FPD. The efficiency of GO is much lower than that of Fe₃O₄ NPs. Since GO is a single-layered material, its surface area is much larger compared to that of the Fe₃O₄ NPs. The fact that Fe₃O₄ still produced stronger fluorescence indicates that Fe₃O₄ NPs are optimal for catalyzing this reaction. The exact mechanism for favoring Fe₃O₄ remains unclear. It might be related to

the preferential binding of the dopamine catechol groups to the Fe^{3+} sites on the Fe_3O_4 NPs.³³

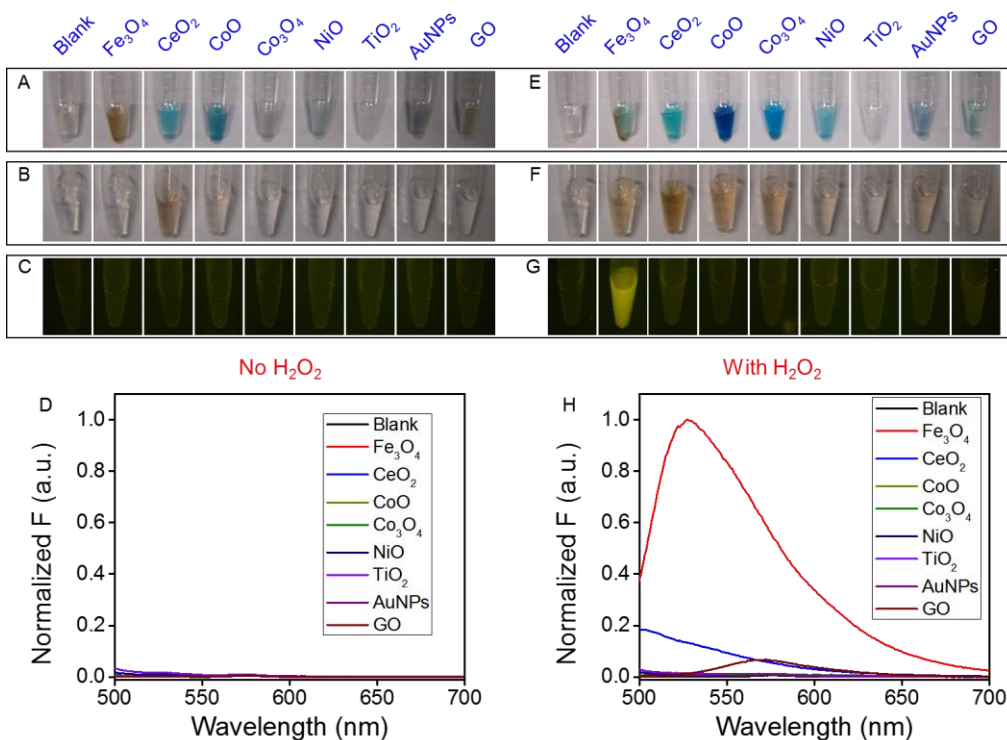


Figure 2. Images of oxidized TMB (A, E), and oxidized dopamine (B, F) under visible light, and the fluorescence of oxidized dopamine under 470 nm excitation (C,G). Fluorescent spectra of dopamine incubated with these nanomaterials (D) in the absence of H_2O_2 and (H) in the presence of H_2O_2 . The concentration of metal oxides was $500 \mu\text{g/mL}$, AuNPs = 5 nM , and graphene oxide = 0.2 mg/mL . The reactions shown in (A-D) and (E-H) panels were carried out in the absence and presence of H_2O_2 , respectively. The TMB (0.5 mM) or dopamine (0.5 mM) oxidation reactions were carried out at pH 4 (acetate buffer, 50 mM) in the presence of optional 20 mM and 5 mM H_2O_2 , respectively. The images were taken after 30 min of reaction.

Nanozyme recycling

One concern of using NPs to catalyze dopamine oxidation is surface deactivation by forming a polydopamine shell. For example, dopamine was reported to form a fluorescent shell on other materials such as SiO₂ and CaCO₃.⁶ In general, dopamine has strong affinity to many surfaces,² and it can even stabilize iron oxide NPs.³³ To test whether a surface coating is formed in our system, we examined the recycling ability of Fe₃O₄ NPs in producing FPD. The fluorescence intensity of the oxidization products after ten reaction cycles still remained 90% of the value of the fresh Fe₃O₄ NPs (Figure 3A). Such high reusability of Fe₃O₄ NPs argues against surface deactivation. TEM also failed to show any observable polymer shell features on the Fe₃O₄ NPs after the dopamine oxidation reaction, further supporting the lack of product adsorption (Figure 3B). Finally, Fe₃O₄ is a strong fluorescence quencher,^(cite your arsenate Chem. Commun. Paper) and we expect FDP emission to be quenched if it adsorbed on the particle surface. Taken together, this study also highlights that Fe₃O₄ NPs is a recyclable catalyst with high catalytic turnovers.

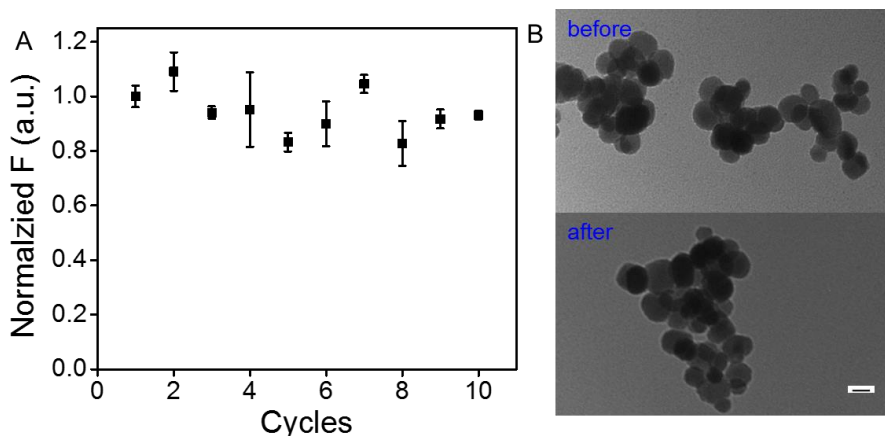


Figure 3. (A) The reusability of Fe₃O₄ NPs in catalyzing dopamine oxidation. The fluorescent intensity 525 nm after each cycle is plotted. The error bars represent standard

deviations from three independent measurements. (B) TEM micrographs of Fe₃O₄ NPs before and after the dopamine oxidation reaction. The scale bar is 20 nm.

Optimization of oxidation conditions

Since the Fe₃O₄ NPs appear to be a highly efficient catalyst for producing FPD, we next aim to further optimize its oxidization reaction. In the same process, we may gain new mechanistic insights. First, the reaction kinetic was studied. The fluorescence spectra of the sample containing dopamine, H₂O₂ and Fe₃O₄ NPs were measured at different time points (Figure 4A). A gradual increase in fluorescence was observed over time, and saturated intensity was reached after 2 h (inset), which is faster than the previous protocols taking 5 h.⁵ The emission peaks showed a slight blue shift in this process, suggesting the breaking down of FPD into smaller molecular weight products with continuous reaction.

The nanozyme activity might also be affected by temperature. Compared to natural enzymes, which work optimally at the body temperature, an advantage of nanozymes is stability over a wide temperature range. We carried out the reaction at different temperatures and recorded the fluorescence spectra after 1 h reaction (Figure 4B). The highest activity was exhibited at 65 °C. At even higher temperature, the fluorescence yield dropped, possibly due to non-specific breaking down or evaporation of H₂O₂ (note that we only used 5 mM H₂O₂).

The effect of pH on the production of FPD was examined next. Fe₃O₄ NPs had the highest efficiency at pH 4 (Figure 4C). This pH optimum is consistent with the peroxidase-like activity of Fe₃O₄ previously reported by other groups.^{20,22} Therefore, it further supports the role of Fe₃O₄ NPs as a peroxidase. It is also interesting to note the catalytic effect of

Fe₃O₄ NPs occurred at all pH's up to pH 8.5 we tested (Figure S7). Therefore, this reaction can also be carried out under physiological conditions with slightly lower efficiency.

Finally, the effect of ionic strength was tested. We incubated dopamine, H₂O₂, and Fe₃O₄ NPs at various NaCl concentrations and measured the resulting UV-vis absorption and fluorescence spectra (excitation 480 nm). The presence of NaCl enhanced dopamine oxidation as indicated by the increase of the absorption peak at 450 nm (Figure S8). The fluorescence of the oxidized dopamine also increased by ~2-fold (Figure 4D). Fe₃O₄ NPs are positively charged at pH 4 (Figure S9), and dopamine has a basic amino group that is protonated at pH 4. Therefore, they experience an electrostatic repulsion at pH 4. A high salt concentration can better screen the charge repulsion between Fe₃O₄ NPs and dopamine, thus facilitating the oxidation reaction. Further adding MgCl₂ did not affect the oxidation reaction, suggesting that NaCl is sufficient for charge screening. Therefore, NaCl (50 mM) was included from this point on.

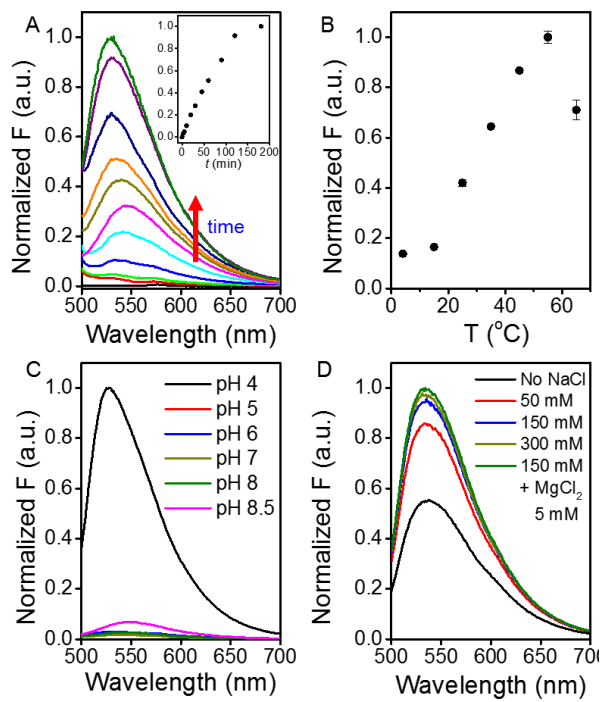


Figure 4. Optimization of reaction conditions for synthesizing FPD. (A) Fluorescence spectra of prepared FPD as a function of time. Effect of (B) temperature, (C) pH, and (D) ionic strength on the activity of Fe₃O₄ NPs measured by the FPD emission intensity. The error bars represent standard deviations from three independent measurements.

FPD as a light-up Zn²⁺ sensor.

The above work demonstrated a mild method for producing FPD. Next, we aim to study its preliminary applications. Rich in hydroxyl group and amino group, dopamine and polydopamine are good metal ligands. Thus they might sense certain metal ions based on the fluorescence property change. For example, Tseng and co-workers reported that their FPD emitting at 440 nm can be specifically quenched by Fe³⁺.⁸ In the presence of 50 μM Fe³⁺, the fluorescence dropped by about 50%, which was proposed for Fe³⁺ sensing. However, such ‘light-off’ sensors are prone to false results with limited room of signal change. The structure of non-fluorescent polydopamine has been a topic of extensive debate,³⁴ and the structures responsible for fluorescence and the effect of metal ions remain unclear.

Before testing our FPD, we examined the stability of FPD against pH, salt concentration, and alkaline metal ions. The fluorescence was quite stable after overnight incubation (Figure S10). We next tested our FPD with different metal ions, and the fluorescence (excited by 470 nm LED) was not significantly quenched by any tested metal ion, including Fe³⁺ (Figure 5A top panel, and Figure 5B).

When excited by a UV lamp at 360 nm (Figure 5A bottom panel), most samples appeared non-fluorescent. This is consistent with 480 nm being the optimal excitation

(Figure S2). Interestingly, a strong blue emission was observed only in the presence of Zn^{2+} . Pb^{2+} also resulted a slightly emission. The fluorescence spectra (Figure 5C) show a strong fluorescence peak at ~ 500 nm in the presence of Zn^{2+} . Therefore, the species that fluoresce by the 480 nm excitation is insensitive to metal ions, while another species is responsible for Zn^{2+} binding. Enhancing the fluorescence yield of organic molecules by Zn^{2+} has been extensively reported and reviewed, and most are related to photo-induced electron or charge transfer.³⁵ We noticed a red shift in the emission peak from 470 nm to 500 nm upon Zn^{2+} binding (Figure 5C). This suggests that the Zn^{2+} sensing might be related to the photo-induced charge transfer (PCT). The fact that Zn^{2+} was only sensed by the shorter excitation wavelength suggests that a less conjugated FPD is required, possibly to provide necessary chemical structures for charge transfer. With such an enhancement effect, we reason that a fluorescence “turn-on” sensor may be developed for Zn^{2+} . Zn^{2+} is an important metal both in the environment and in biology, and extensive efforts have been made for Zn^{2+} detection.^{35,36}

We examined the kinetics of fluorescence enhancement. A fast fluorescence increase after adding Zn^{2+} was observed, reaching the plateau within 3 min (Figure 5D). We then plotted the fluorescence intensity at 500 nm as function of Zn^{2+} concentration (Figure 5E). A linear trend was obtained up to 5 μM Zn^{2+} . The limit of detection (LOD) was calculated to be 60 nM ($\text{LOD} = 3\sigma/\text{slope}$), where σ is the standard deviation of the background. This performance compares favorably with other small molecule based Zn^{2+} sensors.³⁵ Note that the measurement was performed in a complex mixture. It is likely that the sensitivity can be further improved by using the sensitive species alone. Furthermore,

we tested the Zn^{2+} detection in diluted serum (Figure S11). A calibration curve was also successfully obtained with a LOD of 600 nM Zn^{2+} .

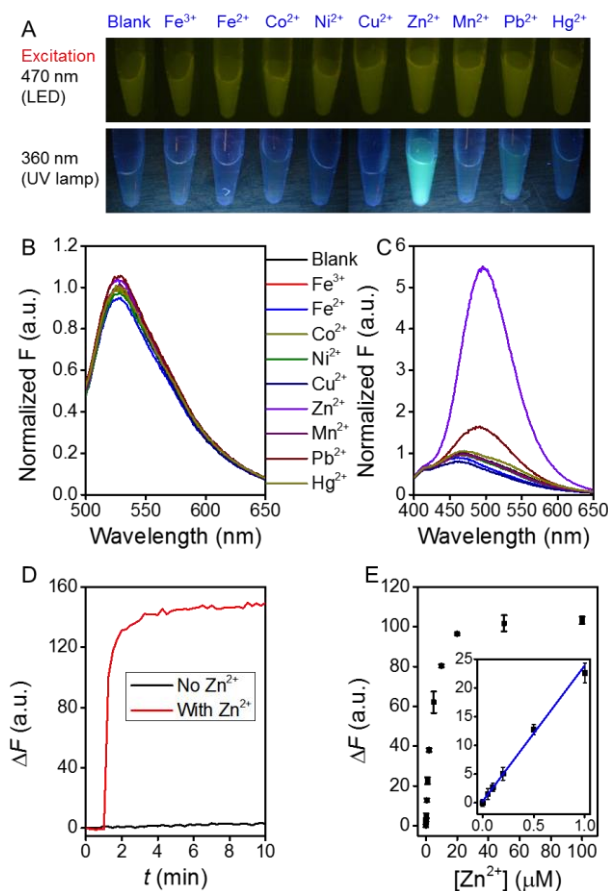


Figure 5. Detection of Zn^{2+} using FPD. (A) Fluorescence images of FPD in the presence of various metal ions (10 μM) under two excitation wavelengths (470 nm and 360 nm). The corresponding fluorescent spectra under (B) 470 nm and (C) 360 nm excitation, respectively. (D) Kinetics of fluorescence variation upon adding Zn^{2+} . (E) Fluorescence intensity as a function of Zn^{2+} concentration. Inset shows the linear part with a fitting line. The error bars represent standard deviations from three independent measurements.

Conclusion

In summary, we demonstrated an efficient nanozyme-assisted method for preparing FPD under mild conditions. The catalysis is likely related to the peroxidase-like activity of Fe₃O₄ NPs. While a few NPs can mimic oxidases (directly oxidizing dopamine without H₂O₂), and most tested nanomaterials have peroxidase-like activity, the preparation of FPD is the best with Fe₃O₄ NPs. Therefore, the ability for oxidation is not the only criteria for the production of FPD. The FPD did not coat the Fe₃O₄ surface to inhibit its further reaction, and the nanozyme can be recycled for 10 times still retaining nearly full activity. The reaction conditions have been optimized in terms of time, temperature, pH and ionic strength, and these optimization efforts also provide new fundamental insights. Finally, we achieved highly sensitive Zn²⁺ detection based on the fluorescence enhancement of FPD at 360 nm excitation (but not with 470 nm excitation). In this case, only a sub-population of the product is sensitive to Zn²⁺. This work indicates that a lot remains to be explored on polydopamine in terms of synthesis, characterization, and application. Nanozymes might play a unique role in this process based on their surface chemistry, robustness, and high catalytic efficiency. This work has found a new direction of using nanozymes for making new materials. This should be a promising application since nanozymes can survive harsh conditions that might be required for such synthesis.

Acknowledgement

Funding for this work is from the Natural Science and Engineering Research Council of Canada (NSERC). H. Xiao is supported by a Chinese Scholarship Council (CSC) scholarship.

Electronic Supplementary Information (ESI) available: [methods, TEM, ζ -potential, and original fluorescence spectra]. See DOI: 10.1039/

References

1. Y. Liu, K. Ai and L. Lu, *Chem. Rev.*, 2014, **114**, 5057-5115.
2. H. Lee, S. M. Dellatore, W. M. Miller and P. B. Messersmith, *Science*, 2007, **318**, 426-430.
3. K. Liu, W.-Z. Wei, J.-X. Zeng, X.-Y. Liu and Y.-P. Gao, *Anal. Bioanal. Chem.*, 2006, **385**, 724-729.
4. C. K. K. Choi, J. Li, K. Wei, Y. J. Xu, L. W. C. Ho, M. Zhu, K. K. W. To, C. H. J. Choi and L. Bian, *J. Am. Chem. Soc.*, 2015, **137**, 7337-7346.
5. X. Zhang, S. Wang, L. Xu, L. Feng, Y. Ji, L. Tao, S. Li and Y. Wei, *Nanoscale*, 2012, **4**, 5581-5584.
6. X. Chen, Y. Yan, M. Müllner, M. P. van Koeveden, K. F. Noi, W. Zhu and F. Caruso, *Langmuir*, 2014, **30**, 2921-2925.
7. A. Yildirim and M. Bayindir, *Anal. Chem.*, 2014, **86**, 5508-5512.
8. J.-H. Lin, C.-J. Yu, Y.-C. Yang and W.-L. Tseng, *Phys. Chem. Chem. Phys.*, 2015, **17**, 15124-15130.
9. N. A. Kotov, *Science*, 2010, **330**, 188-189.
10. H. Wei and E. Wang, *Chem. Soc. Rev.*, 2013, **42**, 6060-6093.
11. Y. Lin, J. Ren and X. Qu, *Acc. Chem. Res.*, 2014, **47**, 1097-1105.
12. X. Wang, Y. Hu and H. Wei, *Inorg. Chem. Front.*, 2016, **3**, 41-60.
13. M. Comotti, C. Della Pina, R. Matarrese and M. Rossi, *Angew. Chem. Int. Ed.*, 2004, **43**, 5812-5815.
14. X. Zheng, Q. Liu, C. Jing, Y. Li, D. Li, W. Luo, Y. Wen, Y. He, Q. Huang, Y.-T. Long and C. Fan, *Angew. Chem. Int. Ed.*, 2011, **50**, 11994-11998.
15. Y. Liu, H. Wu, M. Li, J.-J. Yin and Z. Nie, *Nanoscale*, 2014, **6**, 11904-11910.
16. Y. Song, X. Wang, C. Zhao, K. Qu, J. Ren and X. Qu, *Chem. – Eur. J.*, 2010, **16**, 3617-3621.
17. Y. Song, K. Qu, C. Zhao, J. Ren and X. Qu, *Adv. Mater.*, 2010, **22**, 2206-2210.
18. H. Sun, A. Zhao, N. Gao, K. Li, J. Ren and X. Qu, *Angew. Chem. Int. Ed.*, 2015, **54**, 7176-7180.
19. C. Xu and X. Qu, *NPG Asia Mater.*, 2014, **6**, e90.
20. L. Gao, J. Zhuang, L. Nie, J. Zhang, Y. Zhang, N. Gu, T. Wang, J. Feng, D. Yang, S. Perrett and X. Yan, *Nat. Nanotechnol.*, 2007, **2**, 577-583.
21. B. Liu, Z. Sun, P.-J. J. Huang and J. Liu, *J. Am. Chem. Soc.*, 2015, **137**, 1290-1295.
22. B. Liu and J. Liu, *Nanoscale*, 2015, **7**, 13831-13835.

23. Y. Zhang, Z. Wang, X. Li, L. Wang, M. Yin, L. Wang, N. Chen, C. Fan and H. Song, *Adv. Mater.*, 2016, **28**, 1387-1393.
24. I. Celardo, J. Z. Pedersen, E. Traversa and L. Ghibelli, *Nanoscale*, 2011, **3**, 1411-1420.
25. M. Liang, K. Fan, Y. Pan, H. Jiang, F. Wang, D. Yang, D. Lu, J. Feng, J. Zhao, L. Yang and X. Yan, *Anal. Chem.*, 2013, **85**, 308-312.
26. J. Zhuang, J. Zhang, L. Gao, Y. Zhang, N. Gu, J. Feng, D. Yang and X. Yan, *Mater. Lett.*, 2008, **62**, 3972-3974.
27. H. Wei and E. Wang, *Anal. Chem.*, 2008, **80**, 2250-2254.
28. D. Duan, K. Fan, D. Zhang, S. Tan, M. Liang, Y. Liu, J. Zhang, P. Zhang, W. Liu, X. Qiu, G. P. Kobinger, G. Fu Gao and X. Yan, *Biosens. Bioelectron.*, 2015, **74**, 134-141.
29. E. Golub, H. B. Albada, W.-C. Liao, Y. Biniuri and I. Willner, *J. Am. Chem. Soc.*, 2016, **138**, 164-172.
30. A. Asati, S. Santra, C. Kaittanis, S. Nath and J. M. Perez, *Angew. Chem. Int. Ed.*, 2009, **121**, 2344-2348.
31. J. Liu and Y. Lu, *Nat. Protoc.*, 2006, **1**, 246-252.
32. Y. Tan, W. Deng, Y. Li, Z. Huang, Y. Meng, Q. Xie, M. Ma and S. Yao, *J. Phys. Chem. B*, 2010, **114**, 5016-5024.
33. Y. Liu, D. L. Purich, C. Wu, Y. Wu, T. Chen, C. Cui, L. Zhang, S. Cansiz, W. Hou, Y. Wang, S. Yang and W. Tan, *J. Am. Chem. Soc.*, 2015, **137**, 14952-14958.
34. D. R. Dreyer, D. J. Miller, B. D. Freeman, D. R. Paul and C. W. Bielawski, *Langmuir*, 2012, **28**, 6428-6435.
35. P. Jiang and Z. Guo, *Coord. Chem. Rev.*, 2004, **248**, 205-229.
36. J. Peng, W. Xu, C. L. Teoh, S. Han, B. Kim, A. Samanta, J. C. Er, L. Wang, L. Yuan, X. Liu and Y.-T. Chang, *J. Am. Chem. Soc.*, 2015, **137**, 2336-2342.